Anisotropic H_{c2} of $K_{0.8}Fe_{1.76}Se_2$ determined up to 60 T

E. D. Mun, M. M. Altarawneh, C. H. Mielke, and V. S. Zapf

National High Magnetic Field Laboratory, Los Alamos National Laboratory, Los Alamos, New Mexico 87545, USA

R. Hu, S. L. Bud'ko, and P. C. Canfield

Ames Laboratory, US DOE and Department of Physics and Astronomy, Iowa State University, Ames, Iowa 50011, USA

The anisotropic upper critical field, $H_{c2}(T)$, curves for $K_{0.8}Fe_{1.76}Se_2$ are determined over a wide range of temperatures down to 1.5 K and magnetic fields up to 60 T. Anisotropic initial slopes of $H_{c2} \sim -1.4$ T/K and -4.6 T/K for magnetic field applied along c axis and ab plane, respectively, were observed. Whereas the c axis $H_{c2}^c(T)$ increases quasilinearly with decreasing temperature, the ab plane $H_{c2}^{ab}(T)$ shows a flattening, starting near 25 K above 30 T. This leads to a nonmonotonic temperature dependence of the anisotropy parameter $\gamma_H \equiv H_{c2}^{ab}/H_{c2}^c$. The anisotropy parameter is ~ 2 near $T_c \sim 32$ K and rises to a maximum $\gamma_H \sim 3.6$ around 27 K. For lower temperatures, γ_H decreases with T in a linear fashion, dropping to $\gamma_H \sim 2.5$ by $T \sim 18$ K. Despite the apparent differences between the $K_{0.8}Fe_{1.76}Se_2$ and $(Ba_{0.55}K_{0.45})Fe_2As_2$ or $Ba(Fe_{0.926}Co_{0.074})_2As_2$, in terms of the magnetic state and proximity to an insulating state, the $H_{c2}(T)$ curves are remarkably similar.

Since the discovery of superconductivity in the FeAs-based family, intensive research efforts have focused on finding Fe-based superconductors with a higher transition temperature, T_c, and clarifying the pairing mechanism of superconductivity.[1–6] As additional families have been discovered, the Fe-based superconductors have been categorized into several types including 11 type (P4/nmm, FeSe), 122 type (I4/mmm, AFe_2As_2, $A =$ K, Sr, Ba), and 1111 type (P4/nmm, RFeAsO, $R =$ rare earth). Among these, FeSe is a simple binary system with $T_c \sim 8$ K that can be increased up to 37 K by external pressure.[7] Very recently, higher T_c values (>30 K) were successfully achieved by adding A (K, Rb, Cs, and Tl)[8–11] between the Fe_2Se_2 layers, changing the structure from the 11 type (P4/nmm) to the 122 type (I4/mmm). The discovery of superconductivity in $K_{1-x}Fe_{2-y}Se_2$[8] materials with the same $ThCr_2Si_2$ crystal structure as $BaFe_2As_2$ has given rise to a multitude of measurements, theories, and questions. Even with the dramatically different transport properties (much closer to semiconducting in temperature dependence and absolute value) and magnetic states (antiferromangetism existing up to above 500 K in samples that superconduct near 30 K)[12–15] as compared to superconducting samples of doped $BaFe_2As_2$, the measured magnetic and transport anisotropy is modest[16] and T_c values are comparable to K- and Co-doped members of the $BaFe_2As_2$ family. With these conspicuous differences, and clear similarities, it is of interest to establish the anisotropic upper critical field, $H_{c2}(T)$, curves to see if they are similar to or different from those found in the isostructural FeAs-based 122-type materials. In this communication, high-magnetic-field measurements of radiofrequency (rf) contactless penetration depth into the mixed state are presented and the anisotropic H_{c2} curves for $K_{0.8}Fe_{1.76}Se_2$ are inferred. These results are compared with our earlier measurements of the anisotropic $H_{c2}(T)$ curves for K- and Co-doped $BaFe_2As_2$.[17–20]

The single crystals of $K_{0.8}Fe_{1.76}Se_2$ were grown from a high temperature melt and the actual composition was determined using wavelength dispersive x-ray spectroscopy (WDS). Details of sample growth and characterization are given in Ref. 16. The temperature and magnetic-field dependences of the electrical resistance were measured using the four-probe ac ($f =$ 16 Hz) technique in a Physical Property Measurement System (Quantum Design). To investigate the upper critical-field anisotropy to higher fields ($H \leqslant 60$ T), the magnetic-field dependence of radiofrequency (rf) contactless penetration depth was measured for applied field both parallel ($\mathbf{H} \parallel \mathbf{c}$) and perpendicular ($\mathbf{H} \parallel \mathbf{ab}$) to the tetragonal c axis. The rf contactless penetration depth measurements were performed in a 60-T short-pulse magnet with a 10-ms rise and 40-ms decay time. The rf technique has proven to be a sensitive and accurate method for determining the H_{c2} of superconductors.[21] This technique is highly sensitive to small changes in the rf penetration depth (~ 1–5 nm) in the mixed state. As the magnetic field is applied, the probe detects the transition to the normal state by tracking the shift in resonant frequency, which is proportional to the change in penetration depth as $\Delta\lambda \propto \Delta F/F_0$, where F_0 is 25 MHz in the current setup. Because of the eddy current heating caused by the pulsed field, small single crystals were chosen, where the sample was placed in a circular detection coil for $\mathbf{H} \parallel \mathbf{ab}$ and was located on the top surface of one side of the counterwound coil pair for $\mathbf{H} \parallel \mathbf{c}$.[22,23] For the $\mathbf{H} \parallel \mathbf{c}$ configuration, the coupling between sample and coil is weaker than that for $\mathbf{H} \parallel \mathbf{ab}$, resulting in a smaller frequency shift that is still sufficient to resolve $H_{c2}(T)$. Details about this technique can be found in Refs. 17, 22 and 23.

Figure 1(a) shows the temperature dependence of the normalized resistivity for the $K_{0.8}Fe_{1.76}Se_2$ sample. A sharp drop, corresponding to the superconducting transition, was observed around 32 K. At high temperatures, the resistance increases with decreasing temperature and exhibits a broad maximum at around 220 K.[16,24] The offset and zero-resistance ($R < 3 \times 10^{-5}\Omega$) temperatures were estimated to be $T_c^{\text{offset}} \simeq 32.2$ K and $T_c^{\text{zero}} \simeq 32$ K, respectively, as shown in Fig. 1(b). The solid lines in Fig. 1(b) are warming curves of the rf shift (ΔF) at $H = 0$ for two different samples. As the temperature decreases, the rf shift suddenly increases at T_c, where $T_c = 32$
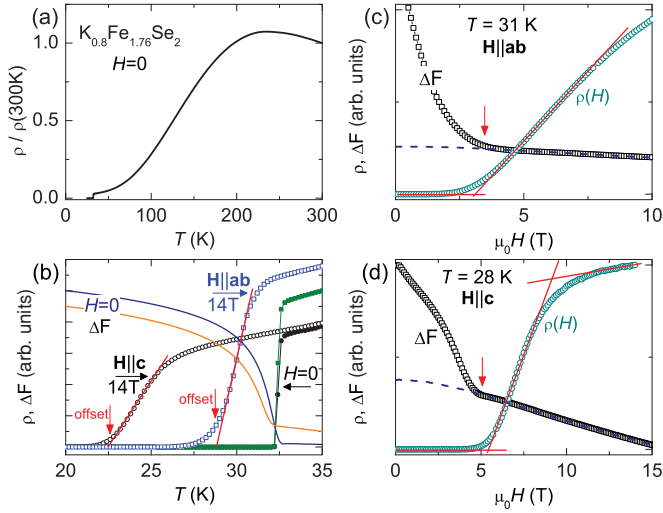
FIG. 1. (Color online) (a) Temperature dependence of the normalized *ab* plane resistivity $\rho(T)$ of the $K_{0.8}Fe_{1.76}Se_2$ single crystal at $H = 0$, where $\rho(300K) = 0.12$ Ω cm.[16] (b) Low-temperature region of the resistance for two samples at $H = 0$ (closed symbols) and 14 T (open symbols) and the warming curves of rf shift (ΔF) for two samples (solid lines). Vertical arrows indicate T_c^{offset} and lines on the top of the 14-T data are guide to the eye. (c) Comparison of the *ab* plane resistance $R(H)$ and ΔF for $\mathbf{H} \parallel \mathbf{ab}$ at $T = 31$ K. (d) Comparison of the *ab* plane resistance $R(H)$ and ΔF for $\mathbf{H} \parallel \mathbf{c}$ at $T = 28$ K. The dashed lines in (c) and (d) are the ΔF taken at $T = 35$ K as a normal-state background signal. The solid lines in (c) and (d) are guides to the eye for offset and onset criteria of H_c and vertical arrows indicate the deviation of ΔF from the background signal (see text).

and 32.4 K for two samples were determined from $d\Delta F/dT$. A clear anisotropy in the response of the superconductivity under applied fields was observed between $\mathbf{H} \parallel \mathbf{ab}$ and $\mathbf{H} \parallel \mathbf{c}$ as shown in Fig. 1(b) for $H = 14$ T curves. To compare the superconducting transition between resistance and the ΔF measurement, resistance data measured in a superconducting magnet and ΔF taken in pulsed magnetic fields at $T = 31$ K for $\mathbf{H} \parallel \mathbf{ab}$ and at $T = 28$ K for $\mathbf{H} \parallel \mathbf{c}$ are plotted in Figs. 1(c) and 1(d), respectively. As shown in the figures, the deviation from the background signal of Δ F is close to the H_c^{offset} criterion of the resistance curves.

Using the deviation from normal-state criterion just discussed, the ΔF versus H plots shown in Figs. 2 and 3 can be used to infer the temperature dependence of the upper critical field $H_{c2}(T)$ by taking the slope of the rf signal intercepting the slope of the normal-state background or by simply taking the first point deviating from the normal-state background. Importantly, the difference between these two related criteria is small and does not affect the $H_{c2}(T)$ curve. In the high-temperature region, the point at which the ΔF signal deviates from the background is close to the H_c^{offset} of the resistance data as shown in Figs. 1(c) and 1(d). Therefore, H_{c2} was determined at the point at which ΔF deviates from the background signal. Arrows in Figs. 2 and 3 indicate the determined H_{c2}. The difference between the H_{c2} values determined by the first deviation and slope-
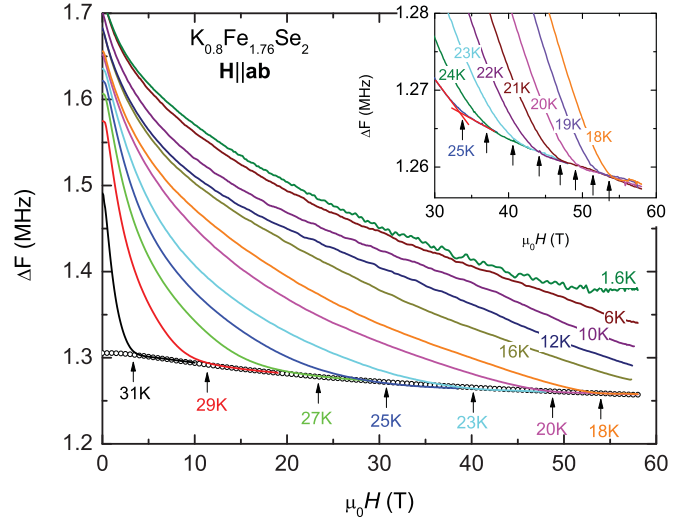

FIG. 2. (Color online) Frequency shift (ΔF) as a function of magnetic field for $\mathbf{H} \parallel \mathbf{ab}$ at selected temperatures. Open symbols are ΔF taken at $T = 35$ K as a normal-state background signal. The arrows indicate H_{c2} determined from the point deviating from background signal. (Inset) The low-temperature data close to H_c. The straight lines on the $T = 25$ K curve are guides to the eye for determining the point at which the rf signal intercepts the slope of the normal-state background.

change point criteria was used to determine the H_{c2} error bar size.

The $H_{c2}(T)$ curves for both $\mathbf{H} \parallel \mathbf{ab}$ (H_{c2}^{ab}) and $\mathbf{H} \parallel \mathbf{c}$ (H_{c2}^c) in $K_{0.8}Fe_{1.76}Se_2$ are plotted in Fig. 4, as determined from the $H \leqslant 14$ T resistance and from the $H \leqslant 60$ T data taken from the down sweep of pulsed-field magnetic-field rf
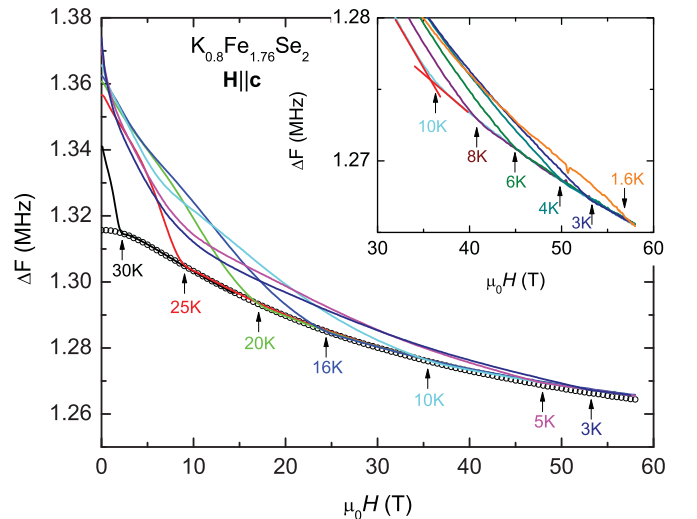

FIG. 3. (Color online) Frequency shift (ΔF) as a function of magnetic field for $\mathbf{H} \parallel \mathbf{c}$ at selected temperatures. Open symbols are ΔF taken at $T = 35$ K as a normal-state background signal. The arrows indicate H_{c2} determined from the point deviating from background signal. (Inset) The low-temperature data close to H_c. The straight lines on $T = 10$ K curve are guides to the eye for determining the point at which the rf signal intercepts the slope of the normal-state background.
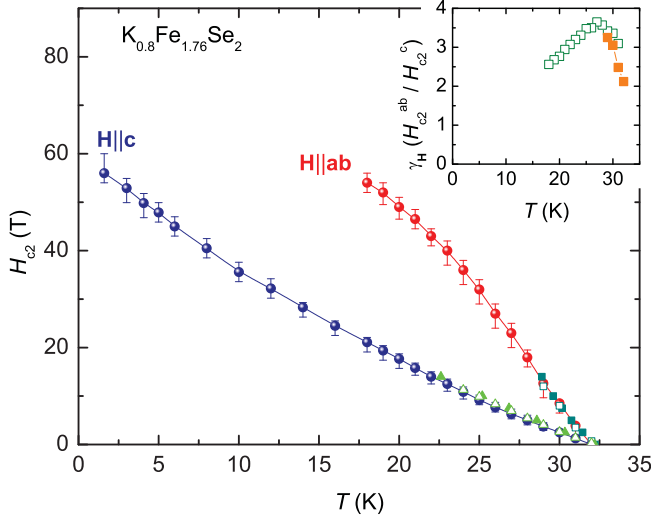
FIG. 4. (Color online) Anisotropic $H_{c2}(T)$ for $K_{0.8}Fe_{1.76}Se_2$ single crystals. Solid circles are obtained from the pulsed-field rf shift measurements and closed (open) square and triangle symbols are taken from temperature (magnetic field)-dependent resistance measurements. (Inset) The temperature dependence of the anisotropy $\gamma_H = H_{c2}^{ab}/H_{c2}^c$ as determined from pulsed-field rf shift (open squares) and resistance (solid squares) measurements.

measurements. The curvature of $H_{c2}(T)$ has been reported to vary depending on the criteria used to determine H_{c2}, for example, in the case of highly two-dimensional, high-T_c cuprate superconductors.[25] In this study, the shape of the H_{c2} curves does not change qualitatively when H_{c2} is defined by different criteria or even different measurements. On the other hand, the shapes of the upper critical field curves for $\mathbf{H} \parallel \mathbf{ab}$ and $\mathbf{H} \parallel \mathbf{c}$ clearly do not manifest the same temperature dependence. As evidenced from Fig. 4, a conventional linear field dependence of H_{c2} is observed close to the T_c, with clearly different slopes for the two field orientations. In the low-field region the H_{c2} curves are consistent with earlier studies.[24,26] Toward higher fields, $H_{c2}^c(T)$ presents an almost linear temperature dependence down to 1.5 K, whereas the curve of $H_{c2}^{ab}(T)$ has a tendency to saturate. The anisotropy parameter, $\gamma_H \equiv H_{c2}^{ab}/H_{c2}^c$, is about ~ 2 near T_c but shows a maximum around 27 K with $\gamma_H \sim 3.6$ and decreases considerably for lower temperatures. In all known examples so far, the temperature dependence of γ_H was opposite to that of $\gamma_\lambda \equiv \lambda_c/\lambda_{ab}$. It would be interesting to examine $\gamma_\lambda(T)$ in this material, in particular, to see if it goes through a minimum at ~ 27 K.

The zero temperature limit of H_{c2} can be estimated by using the Werthamer-Helfand-Hohenberg (WHH) theory,[27] which gives $H_{c2} = 0.69T_c(dH_{c2}/dT)\mid_{T_c}$. The value of $H_{c2}(0)$ for $\mathbf{H} \parallel \mathbf{ab}$ and $\mathbf{H} \parallel \mathbf{c}$ were estimated to be ~ 102 and ~ 31 T, respectively, where $T_c = 32$ K, $dH_{c2}^{ab}/dT \sim -4.6 T/K$, and $dH_{c2}^c/dT \sim -1.4$ T/K were used. Clearly, these values do not capture the salient physics for this compound. On the other hand, in the simplest approximation, the Pauli limit (H_P) is given by $1.84T_c$,[28–30] giving $H_P \sim 59$ T. This low-temperature value of H_{c2} may indeed capture some of the basic physics associated with $K_{0.8}Fe_{1.76}Se_2$. To explain the observed H_{c2} curves in detail, a more complete theoretical treatment is needed, one that does not exclude the strong electron-phonon coupling and multiband nature of Fe-based compounds. Anisotropic superconducting coherence length can be calculated using $H_{c2}^{ab} = \frac{\phi_0}{2\pi\xi_{ab}\xi_c}$ and $H_{c2}^c = \frac{\phi_0}{2\pi\xi_{ab}^2}$.[31] If $H_{c2}^c = 60$ T and H_{c2}^{ab} is assumed to be between 60 and 100 T, then $\xi_{ab} \sim 2.3$ nm and 1.4 nm $\lesssim \xi_c \lesssim 2.3$ nm.

On the basis of this study for $K_{0.8}Fe_{1.76}Se_2$, the behavior of $H_{c2}(T)$ is found to be very similar to that of several 122-type systems as well as doped FeSe.[17–20] It should be noted that the H_{c2} curves for two orientations in the K-doped $BaFe_2As_2$ system seem to cross at low temperatures due to the flattening of $H_{c2}^{ab}(T)$ curve;[17,19] additionally, the H_{c2} curves for $FeTe_{0.6}Se_{0.4}$ shows a crossing between $\mathbf{H} \parallel \mathbf{ab}$ and $\mathbf{H} \parallel \mathbf{c}$ curves below 4.5 K because of the subsequent flattening of the H_{c2}^{ab} curve at low temperatures.[32,33] However, in the Co-doped system, the anisotropic $H_{c2}(T)$ curves do not show such crossing,[18,20] a result similar to what was found in this study. Thus, an intriguing feature of $H_{c2}(T)$ curves for Co- and K-doped $BaFe_2As_2$, $FeTe_{0.6}Se_{0.4}$, and $K_{0.8}Fe_{1.76}Se_2$ systems is that the anisotropy near T_c is as large as 3 but drops toward ~ 1 as $T \to 0$ K. The $H_{c2}(T)$ anisotropy in $K_{0.8}Fe_{1.76}Se_2$ is particularly noteworthy given that it exists deep within an antiferromagnetically ordered state.[13–15] In the case of Co-doped Ba122, $\gamma_H(T) \sim 1$ when $T_c < T_N$ with clear anisotropy emerging only when the antiferromagnetic state is suppressed.[18] These results raise the following question: To what extent is the antiferromagnetism in $K_{0.8}Fe_{1.76}Se_2$ interacting with lower-temperature superconductivity? Clearly more work will be needed to answer this key query.

In summary, the H_{c2}-T phase diagram for the $K_{0.8}Fe_{1.76}Se_2$ has been constructed by means of measuring both the electrical resistance in a dc superconducting magnet ($H \leqslant 14$ T) and the rf contactless penetration depth in a pulsed magnetic field up to 60 T. The upper critical field of $K_{0.8}Fe_{1.76}Se_2$ is determined as $H_{c2}^{ab}(18 \text{ K}) \simeq 54$ T and $H_{c2}^c(1.6 \text{ K}) \simeq 56$ T. The anisotropy parameter γ_H initially increases with decreasing temperature, passes through a maximum of ~ 3.6 near 27 K, and then decreases to ~ 2.5 at 18 K. The observed γ_H values show a weakening anisotropic effect at low temperatures. Although the Fe-based superconductors have a layered crystal structure, a weak anisotropy of H_{c2} may be a common feature, suggesting that the interlayer coupling and the three-dimensional Fermi surface may play an important role in the superconductivity of this family.

[1] Y. Kamihara, T. Watanabe, M. Hirano, and H. Hosono, J. Am. Chem. Soc. **130**, 3296 (2008).

[2] M. Rotter, M. Tegel, and D. Johrendt, Phys. Rev. Lett. **101**, 107006 (2008).

[3] X. C. Wang, Q. Q. Liu, Y. X. Lv, W. B. Gao, L. X. Yang, R. C. Yu, F. Y. Li, and C. Q. Jin, Solid State Commun. **148**, 538 (2008).

[4] F. C. Hsu, J. Y. Luo, K. W. Yeh, T. K. Chen, T. W. Huang, P. M. Wu, Y. C. Lee, Y. L. Huang, Y. Y. Chu, D. C. Yan, and M. K. Wu, Proc. Natl. Acad. Sci. USA **105**, 14262 (2008).

[5] Paul C. Canfield and Sergey L. Bud'ko, Annu. Rev. Condens. Matter Phys. **1**, 27 (2010).

[6] Johnpierre Paglione and Richard L. Greene, Nat. Phys. **6**, 645 (2010).

[7] S. Margadonna, Y. Takabayashi, Y. Ohishi, Y. Mizuguchi, Y. Takano, T. Kagayama, T. Nakagawa, M. Takata, and K. Prassides, Phys. Rev. B **80**, 064506 (2009).

[8] J. Guo, S. Jin, G. Wang, S. Wang, K. Zhu, T. Zhou, M. He, and X. Chen, Phys. Rev. B **82**, 180520 (2010).

[9] J. J. Ying, X. F. Wang, X. G. Luo, A. F. Wang, M. Zhang, Y. J. Yan, Z. J. Xiang, R. H. Liu, P. Cheng, G. J. Ye, and X. H. Chen, e-print arXiv:1012.5552 (2010).

[10] C. H. Li, B. Shen, F. Han, X. Zhu, and H. H. Wen, e-print arXiv:1012.5637 (2010).

[11] M. Fang, H. Wang, C. Dong, Z. Li, C. Feng, J. Chen, and H. Q. Yuan, e-print arXiv:1012.5236 (2010).

[12] Z. Shermadini, A. Krzton-Maziopa, M. Bendele, R. Khasanov, H. Luetkens, K. Conder, E. Pomjakushina, S. Weyeneth, V. Pomjakushin, O. Bossen, and A. Amato, Phys. Rev. Lett. **106**, 117602 (2011).

[13] V. Yu. Pomjakushin, E. V. Pomjakushina, A. Krzton-Maziopa, K. Conder, and Z. Shermadini, e-print arXiv:1102.3380.

[14] W. Bao, G. N. Li, Q. Huang, G. F. Chen, J. B. He, M. A. Green, Y. Qiu, D. M. Wang, J. L. Luo, and M. M. Wu, e-print arXiv:1102.3674.

[15] D. H. Ryan, W. N. Rowan-Weetaluktuk, J. M. Cadogan, R. Hu, W. E. Straszheim, S. L. Bud'ko, and P. C. Canfield, e-print arXiv:1103.0059.

[16] R. Hu, K. Cho, H. Kim, H. Hodovanets, W. E. Straszheim, M. A. Tanatar, R. Prozorov, S. L. Bud'ko, P. C. Canfield, e-print arXiv:1102.1931.

[17] M. M. Altarawneh, K. Collar, C. H. Mielke, N. Ni, S. L. Bud'ko, and P. C. Canfield, Phy. Rev. B **78**, 220505(R) (2008).

[18] N. Ni, M. E. Tillman, J.-Q. Yan, A. Kracher, S. T. Hannahs, S. L. Bud'ko, and P. C. Canfield, Phys. Rev. B **78**, 214515 (2008).

[19] H. Q. Yuan, J. Singleton, F. F. Balakirev, S. A. Baily, G. F. Chen, J. L. Luo, and N. L. Wang, Nature (London) **457**, 565 (2009).

[20] M. Kano, Y. Kohama, D. Graf, F. Balakirev, A. S. Sefat, M. A. McGuire, B. C. Sales, D. Mandrus, and S. W. Tozer, J. Phys. Soc. Jpn. **78**, 084719 (2009).

[21] C. Mielke, J. Singleton, M.-S. Nam, N. Harrison, C. C. Agosta, B. Fravel, and L. K. Montgomery, J. Phys. Condens. Matter **13**, 8325 (2001).

[22] T. Coffey, Z. Bayindir, J. F. DeCarolis, M. Bennett, G. Esper, and C. C. Agosta, Rev. Sci. Instrum. **71**, 4600 (2000).

[23] M. M. Altarawneh, C. H. Mielke, and J. S. Brooks, Rev. Sci. Instrum. **80**, 066104 (2009).

[24] Y. Mizuguchi, H. Takeya, Y. Kawasaki, T. Ozaki, S. Tsuda, T. Yamaguchi, and Y. Takano, Appl. Phys. Lett. **98**, 042511 (2011).

[25] Y. Ando, G. S. Boebinger, A. Passner, L. F. Schneemeyer, T. Kimura, M. Okuya, S. Watauchi, J. Shimoyama, K. Kishio, K. Tamasaku, N. Ichikawa, and S. Uchida, Phys. Rev. B **60**, 12475 (1999).

[26] D. M. Wang, J. B. He, T.-L. Xia, G. F. Chen, e-print arXiv:1101.0789.

[27] N. R. Werthamer, E. Helfand, and P. C. Hohemberg, Phys. Rev. **147**, 295 (1966).

[28] A. M. Clogston, Phys. Rev. Lett. **9**, 266 (1962).

[29] B. S. Chandrasekhar, Appl. Phys. Lett. **1**, 7 (1962).

[30] K. Maki, Phys. Rev. **148**, 362 (1966).

[31] Charles P. Poole, Jr., (ed.), *Handbook of Superconductivity* (Academic Press, San Diego, CA, 2000).

[32] S. Khim, J. W. Kim, E. S. Choi, Y. Bang, M. Nohara, H. Takagi, and K. H. Kim, Phys. Rev. B **81**, 184511 (2010).

[33] M. H. Fang, J. H. Yang, F. F. Balakirev, Y. Kohama, J. Singleton, B. Qian, Z. Q. Mao, H. D. Wang, and H. Q. Yuan, Phys. Rev. B **81**, 020509(R) (2010).